Improving qBOLD based measures of oxygen extraction fraction using hyperoxia-BOLD derived measures of blood volume

Alan J Stone[1,2,3,4], Nicholas P Blockley[1,5]

[1]Wellcome Centre for Integrative Neuroimaging, FMRIB, Nuffield Department of Clinical Neurosciences, University of Oxford, Oxford, United Kingdom

[2]Department of Medical Physics and Clinical Engineering, Beaumont Hospital, Dublin, Ireland

[3]National Neuroscience Centre, Beaumont Hospital, Dublin, Ireland

[4]Centre for Physics and Health in Medicine, School of Physics, University College Dublin, Dublin, Ireland

[5]School of Life Sciences, University of Nottingham, United Kingdom

Running title: Improving qBOLD measures of OEF using hyperoxia-BOLD

Word count: 5158 (max 5000)

Figures: 6 figures + 4 tables (max 10)

References: 45

Address for correspondence: Nicholas Blockley, School of Life Sciences, The University of Nottingham Medical School, Queen's Medical Centre, Nottingham, NG7 2UH, UK

E-mail address: nicholas.blockley@nottingham.ac.uk

Abstract (max 250 words)

Purpose: Streamlined-qBOLD (sqBOLD) is a refinement of the quantitative BOLD (qBOLD) technique capable of producing non-invasive and quantitative maps of oxygen extraction fraction (OEF) in a clinically feasible scan time. However, sqBOLD measurements of OEF have been reported as being systematically lower than expected in healthy brain. Since the qBOLD framework infers OEF from the ratio of the reversible transverse relaxation rate (R_2') and deoxygenated blood volume (DBV), this underestimation has been attributed the overestimation of DBV. Therefore, this study proposes the use of an independent measure of DBV using hyperoxia-BOLD and investigates whether this results in improved estimates of OEF.

Methods: Monte Carlo simulations were used to simulate the qBOLD and hyperoxia-BOLD signals and to compare the systematic and noise related errors of sqBOLD and the new hyperoxia-qBOLD (hqBOLD) technique. Experimentally, sqBOLD and hqBOLD measurements were performed and compared with TRUST (T_2 relaxation under spin tagging) based oximetry in the sagittal sinus.

Results: Simulations showed a large improvement in the uncertainty of DBV measurements leading to a much improved dynamic range for OEF measurements with hqBOLD. In a group of ten healthy volunteers, hqBOLD produced measurements of OEF in cortical grey matter (OEF_{hqBOLD} = 38.1 ± 10.1 %) that were not significantly different to TRUST oximetry measures (OEF_{TRUST} = 40.4 ± 7.7 %), whilst sqBOLD derived measures (OEF_{sqBOLD} = 16.1 ± 3.1 %) were found to be significantly different.

Conclusion: The simulations and experiments in this study demonstrate that an independent measure of DBV provides improved estimates of OEF.

Introduction

Oxygen extraction fraction (OEF) is an important indicator of the metabolic function of brain tissue that describes the fraction of oxygen removed from arterial blood to serve oxidative metabolism. The quantitative BOLD (qBOLD) technique provides the capability to non-invasively and quantitatively map OEF on a regional level[1,2]. Streamlined-qBOLD (sqBOLD) is a refinement of this approach that seeks to simplify the acquisition and analysis of data to provide a more clinically relevant approach[3].

Measurements of OEF using sqBOLD are lower than expected when compared with literature values (OEF_{sqBOLD} ~ 20%, $OEF_{literature}$ ~ 30 - 40%)[3]. Since OEF is derived from the ratio of the irreversible transverse relaxation rate (R_2') and the deoxygenated blood volume (DBV), it follows that the underestimation of OEF could be due to underestimation of R_2' or overestimation of DBV. The sqBOLD technique utilises an asymmetric spin echo (ASE) acquisition, with which R_2' has been measured to be in the range of 2.6–3.6 s^{-1} in grey matter (GM)[3–5]. This is consistent with previous ASE measurements[6] of 3.5 s^{-1} and with different acquisitions such as gradient echo sampling of spin echo (GESSE)[2] measuring 2.9 s^{-1}. DBV has been measured by sqBOLD to be in the range 3.6–6.7 % in GM[3–5]. This is consistent with other ASE based measurements[6] of 4.3 %, but not with previous measurements using GESSE[2] of 1.8 % or hyperoxia-BOLD[7] of 2.2 %, suggesting that DBV overestimation might be responsible for OEF underestimation in ASE based qBOLD. This hypothesis is given further weight by simulations of ASE based qBOLD showing that diffusion, which is not incorporated in the qBOLD model, causes DBV to be overestimated[8]. There is therefore great potential to improve the accuracy of sqBOLD by improving the accuracy of DBV measurements.

Multiparametric qBOLD (mq-BOLD) introduced the concept of acquiring an independent measurement of blood volume which is combined with a measurement of R_2' acquired from separate maps[9,10] of T_2 and T_2^*. Here the blood volume is measured using the dynamic susceptibility contrast (DSC) technique[11] which requires an injection of a Gadolinium-based

contrast agent. However, the DBV in the qBOLD model explicitly refers to the proportion of the blood volume that contains deoxyhaemoglobin. Whereas DSC is sensitive to all of the vascular compartments that the contrast agent passes through and hence is a measure of total cerebral blood volume (CBVt). Therefore, for sqBOLD this DSC measure of CBV would likely drive OEF estimates even lower.

Hyperoxia-BOLD provides an alternative to DSC which is targeted specifically at measuring venous CBV (CBVv). It has been shown that the fractional change in the BOLD signal in response to the administration of oxygen is specific to CBVv and can be scaled to provide quantitative estimates using a heuristic model[7]. The hyperoxia-BOLD and qBOLD techniques rely on the same BOLD contrast. The former uses oxygen as a contrast agent by manipulating the concentration of deoxyhaemoglobin in the deoxygenated blood vessels, whilst the latter relies on the additional signal attenuation due to deoxyhaemoglobin at short ASE refocussing offset times. Therefore, theoretically the CBVv from hyperoxia-BOLD is equivalent to DBV from qBOLD and henceforth we will refer to both as DBV.

The aim of this study is to investigate the use of hyperoxia-BOLD to improve the accuracy of OEF measurements. Firstly, detailed simulations of the proposed technique were performed using a Monte Carlo based approach[8]. The potential for systematic error due to physiological variability and the effect of noise were both examined and compared with ASE based qBOLD. Secondly, experimental measurements were performed to compare the existing sqBOLD approach with the new hyperoxia-qBOLD (hqBOLD) technique. Furthermore, comparison is made of both techniques with whole brain oximetry measurements from the TRUST (T_2 relaxation under spin tagging) technique[12].

Methods

Simulations

Simulations of the qBOLD and hyperoxia-BOLD signal were performed using a previously reported approach[8]. A brief summary of this approach follows. Monte Carlo simulations of the random walk of protons around deoxygenated blood vessels modelled as infinite cylinders were performed using a standard approach[13] for a range of different vessel radii and nominal oxygenation at 3 T. The resulting phase accrual was saved for each proton in 2 ms intervals for a total of 120 ms. The ASE signal is then generated by summing the phase accrued prior to the refocussing pulse and subtracting the phase accrued following the refocussing pulse. Whilst the gradient echo (GRE) signal is produced by summing the phase accrued up to the required TE. These data can be scaled to the target oxygenation[14] prior to summation of the individual proton's phases to simulate the extravascular signal. This extravascular signal is then used to estimate a radius dependent shape function enabling the signal to be scaled to the target blood volume fraction[15]. To account for the range of vessel radii encountered *in vivo*, the extravascular signal from multiple vessel radii can be combined as the product of single radii simulations[15,16]. A discrete model of the cerebral vasculature was used to select these radii[17]. Finally, the intravascular signal is simulated using an analytical model of the blood signal[18,19].

In this study, simulations of the ASE qBOLD and GRE BOLD signals were performed to match the experimental parameters described in later sections. Due to the limitations of the existing Monte Carlo data, the simulated spin echo displacement times (τ) of the ASE measurements were required to be a multiple of 4 ms and the TE of the BOLD measurements a multiple of 2 ms. Since the experimental values did not meet these criteria a wider range of τ and TE values were simulated and linearly interpolated to the required values. The hyperoxia-BOLD experiment was simulated by estimating the oxygen carrying capacity (CaO_2) of arterial blood during normoxia and hyperoxia,

$$CaO_2 = \phi[Hb]SaO_2 + \varepsilon PaO_2 \qquad (1)$$

where the constant ϕ is the oxygen carrying capacity of haemoglobin (1.34 $mlO_2\ g^{-1}$), [Hb] is the haemoglobin concentration (typical value 15 gHb dl^{-1}), ε is the solubility coefficient of oxygen in plasma (0.0031 $mlO_2\ dl^{-1}\ mmHg^{-1}$) and the arterial oxygen saturation (SaO_2) was estimated using the Severinghaus equation[20]. The amount of oxygen extracted for metabolism ($CmetO_2$) was assumed to be constant for normoxia and hyperoxia, enabling the venous oxygen carrying capacity (CvO_2) to be estimated.

$$CvO_2 = CaO_2 - CmetO_2 = \phi[Hb]SvO_2 + \varepsilon PvO_2 \qquad (2)$$

The venous partial pressure of oxygen (PvO_2) was calculated assuming that the plasma oxygen component was non-negligible and used to calculate the venous oxygen saturation (SvO_2) via the Severinghaus equation. Finally, the capillary oxygen saturation (ScO_2) was calculated as a weighted sum of the SaO_2 and SvO_2 ($ScO_2 = \kappa\ SaO2 + (1-\kappa)\ SvO_2$), with a weighting factor κ=0.4 giving a greater weighting towards venous blood[21,22].

The combined physical and physiological model of the MRI signal was used in two ways: (i) to investigate the presence of systematic error and (ii) to investigate the effect of noise on the parameter estimates. Systematic error was investigated in the absence of system noise and incorporated variations in CBVt, OEF, haematocrit (Hct), normoxic PaO_2 (PaO_2^{norm}) and hyperoxic PaO_2 (PaO_2^{hyper}). As in previous publications, this was achieved by randomly generating values in a predefined range (Table 1) using a uniform random number generator for all five parameters[23]. These values were then used to generate ASE and BOLD signals using the model. This process was repeated to produce 1,000 different physiological states and accompanying signals. These signals were processed to generate estimates of R_2' and OEF using the process described in the analysis section below. The estimation of DBV differed from the experimental method, which uses linear regression, in that single estimates of the BOLD signal at normoxia and hyperoxia were used to calculate the percentage change in the BOLD signal (δBOLD) between these two conditions.

The effect of noise was investigated by simulating signals for standard physiological values (Table 1). Gaussian random noise was then added to these signals before calculating R_2', DBV and OEF. This process was repeated 20,000 times. The SNR for ASE and BOLD was estimated for the whole brain from the experimental data following Method 1 of the National Electrical Manufacturers Association (NEMA) guidelines[24]. For the ASE data two consecutively acquired τ=0 (spin echo) images were used. Across the group, ASE SNR was measured as 52 and for BOLD the SNR was 87. To account for the averaging process inherent in the experimental linear regression analysis, multiple signals with added noise were generated for normoxia and hyperoxia and averaged before calculating δBOLD. This consisted of 100 signal averages during hyperoxia and 100 during normoxia.

For the purposes of comparison, the *true value* of a parameter is required. This is problematic given the definition of DBV as the vascular volume containing deoxygenated blood since this applies to both capillaries and veins. However, the capillaries contain proportionally less deoxyhaemoglobin due to a higher oxygen saturation and generate a smaller fraction of the overall qBOLD signal i.e. the signal from capillaries is expected to increase quadratically with blood oxygenation, but the linear scaling constant is 100 times smaller than for large venous vessels[25]. Therefore, pragmatically DBV is defined as the blood volume within the venous vessels of the model. This is consistent with our previous simulations of the hyperoxia-BOLD signal[7], but not our previous simulations of the qBOLD signal[8]. The true R_2' was then calculated using this definition of DBV,

$$R_2' = \gamma \, \frac{4}{3} \, \pi \, \Delta\chi_0 \, Hct \, OEF \, B_0 \, DBV \qquad (3)$$

where γ is the proton gyromagnetic ratio, $\Delta\chi_0$ is the susceptibility difference between oxygenated and deoxygenated red blood cells ($\Delta\chi_0 = 0.264 \times 10^{-6}$ [26]), B_0 is the main magnetic field (B_0 = 3 T) and the known Hct from the simulations. The true OEF was an input to the simulations.

Imaging

Ten healthy participants (aged 23 – 41; median 29; 3 female, 7 male) were scanned with local ethics committee approval using a 3T Siemens Prisma (Siemens Healthcare, Erlangen, Germany) with a 32-channel receive-only head coil. Figure 1 presents an overview of the imaging data acquired, the parameters derived from this imaging data and the main comparisons performed in this study. MRI data were acquired in the following order:

TRUST oximetry measurements were made in the superior sagittal sinus (SSS) using the following parameters: FOV = 230 mm^2, 64 x 64 matrix, TR / TE = 3 s / 7 ms, flip angle (FA) = 90°, GRAPPA = 3, partial Fourier = 6/8, bandwidth (BW) = 2604 Hz/px, tag-gap = 25 mm, tag-thickness = 100 mm, TI = 1050 ms. Four tag–control pairs were acquired at four different effective echo times (eTE = 0, 40, 80 and 160 ms) resulting in thirty-two acquisitions and a total scan duration of 1:53 mins.

The sqBOLD measurements were made using a FLAIR-GASE acquisition[27,28] with the following parameters: FOV = 220 mm^2, 96 x 96 matrix, nine 5 mm slabs (encoded into four 1.25mm slices, 100% partition oversampling), 2.5 mm gap, TR / TE = 3 s / 80 ms, FA = 90°, BW = 2004 Hz/px, TI_{FLAIR} = 1210 ms, τ = 0 – 66 ms in steps of 3 ms. This resulted in twenty-three τ-weighted acquisitions with a total scan duration of 9:12 mins.

The same ASE data were used for the hqBOLD measurements and complemented with hyperoxia-BOLD data to independently estimate DBV. BOLD-EPI data were acquired with a matched slice prescription to the FLAIR-GASE acquisitions (FOV = 220 mm^2, 96 x 96 matrix, nine 5 mm slices, 2.5 mm gap, TR / TE = 1 s / 35 ms, FA = 65°, BW = 2004 Hz/px). A prospective end-tidal gas targeting system (RespirAct™ Gen 3, Thornhill Research Inc., Toronto, Canada) was used to modulate end-tidal oxygen ($P_{ET}O_2$) between normoxic and hyperoxic (baseline + 300 mmHg) conditions, whilst maintaining isocapnia (a constant

carbon dioxide level). The hyperoxia paradigm lasted 10 minutes during which time 600 volumes were acquired. The respiratory paradigm consisted of three 2 minute blocks of normoxia interleaved with two 2 minute blocks of hyperoxia. The combined acquisition time was 19:12 mins.

An MPRAGE dataset (FOV = 174 mm x 192 mm x 192 mm, 116 x 128 x 128 matrix, TR / TI / TE = 1900 / 904 / 3.74 ms and FA = 8°) was acquired in each subject[29]. To aid in the registration of the FLAIR-GASE to the structural image, an additional set of whole brain GASE data without a FLAIR preparation were acquired with an increased coverage in the z direction and a set of ASE data with τ = 0 to estimate image SNR.

Data Analysis

The following pre-processing and analysis steps were applied to the data acquired in each subject using a combination of tools from the FMRIB Software Library (FSL)[30] and custom scripts written using MATLAB (The Mathworks, Natick, MA).

The tag and control images of the TRUST data were first motion corrected using the FMRIB linear image registration tool (MCFLIRT) (Jenkinson et al., 2002). Pairwise subtraction of the tag-control images was performed and the four repeats at each eTE averaged. Using the difference image at eTE = 0 ms, the four voxels with the highest signal in the SSS were identified to create a region of interest (ROI). Using the SSS ROI, the mean difference signal (ΔS) was extracted for each eTE. To calculate the T_2 of blood (T_{2b}), ΔS is plotted as a function of eTE and fitted to Eq. 4 to obtain the exponent C [12].

$$\Delta S = S_0 e^{eTE\ C} \qquad (4)$$

The T_2 of blood (T_{2b}) was then estimated from C using Eq. 5 and assuming the T_1 of blood (T_{1b}) to be 1624 ms.

$$T_{2b} = \frac{1}{\frac{1}{T_{1b}} - C} \qquad (5)$$

Assuming a value for haematocrit in large vessels (Hct = 0.42)[31], T_{2b} can be converted to SvO_2 using a calibration model[32]. Assuming arterial blood is fully saturated, an estimate of whole brain OEF is given by 1- SvO_2.

For sqBOLD, the four 1.25 mm slices of each slab of the FLAIR-GASE data were averaged to produce nine 5 mm slices, which were then motion corrected using MCFLIRT[33]. A mask of brain tissue was created using the brain extraction tool (BET)[34] and further analysis was restricted to voxels within this mask. The τ-series for each voxel were then fit using a linear system (A · x = B) to simultaneously estimate R_2', DBV and a constant term representing the underlying proton density and T_2 decay[4].

$$\begin{bmatrix} 0 & 0 & 1 \\ \vdots & \vdots & \vdots \\ 1 & -\tau_1 & 1 \\ 1 & -\tau_2 & 1 \\ \vdots & \vdots & \vdots \\ 1 & -\tau_n & 1 \end{bmatrix} \begin{bmatrix} DBV \\ R_2{}' \\ \log(S_0) - TE \cdot R_2 \end{bmatrix} = \begin{bmatrix} \log\big(S(\tau_0)\big) \\ \vdots \\ \log\big(S(\tau_1)\big) \\ \log\big(S(\tau_2)\big) \\ \vdots \\ \log\big(S(\tau_n)\big) \end{bmatrix} \qquad (6)$$

Here, S(τ) is the signal intensity as a function of τ, where τ_0 represents acquisitions at τ = 0 ms and τ_1 to τ_n are values of τ > 15 ms. In matrix A the first row describes the short τ regime relevant to τ_0 and subsequent rows the long τ regime[35] representing τ > 15 ms. The least squares solution was used to produce voxel-wise estimates of R_2' and DBV. Parameter maps of OEF were then calculated using $\Delta\chi_0 = 0.264 \times 10^{-6}$ [26] and small vessel Hct[36] of 0.34.

$$OEF = \frac{R_2'}{DBV\ \gamma \frac{4}{3} \pi\ \Delta\chi_0\ Hct\ B_0} \qquad (7)$$

For the multi-parametric hqBOLD approach, a map of R_2' was calculated from the same data as for sqBOLD but only for images with τ > 15 ms using a log-linear least squares fit for R_2' and the constant term. The hyperoxia-BOLD data were then analysed in the following way. The BOLD data were motion corrected using MCFLIRT and then transformed into the

FLAIR-GASE image space using FLIRT[37]. Measurements of $P_{ET}O_2$ were interpolated onto the 1 sec time resolution of the BOLD data and smoothed to generate a regressor of the blood oxygenation change. This model was fitted to the hyperoxia-BOLD data on a voxel-wise basis using the least squares method and used to calculate the fractional BOLD signal change to hyperoxia (δBOLD). The change in $P_{ET}O_2$ during the hyperoxia challenge ($\Delta P_{ET}O_2$) was calculated by taking the mean of data within windows during baseline (repetitions 1 to 100) and hyperoxia (repetitions 175 to 225 and 415 to 465). These measurements were used to calculate DBV, under the assumption that $\Delta P_{ET}O_2 = \Delta PaO_2$ (the change in PaO_2) using Eq. 8, where the constant A = 27 ms, B = 0.2, C = 245.1 mmHg, D = 0.1 have been previously described[7].

$$DBV = \left(\frac{A}{TE} + B\right)\left(\frac{C}{\Delta PaO_2} + D\right) \delta BOLD \qquad (8)$$

Regional Analysis

Subject specific ROIs of cortical GM and white matter (WM) were created from the FLAIR-GASE (τ=0) data using FMRIB's automated segmentation tool (FAST)[38] by taking advantage of the T_1-weighting caused by the FLAIR preparation. GM partial volume estimate (PVE) maps were threshold at 50% and further refined to cortical GM by transforming the MNI structural atlas[39] into the FLAIR-GASE space via the MPRAGE using FLIRT. Frontal, insula, occipital, parietal and temporal lobes were included in the cortical mask to produce the final cortical GM ROI. WM ROIs were generated by thresholding the WM PVE maps at 100%.

Statistical testing

A one-way ANOVA was used to test the null hypothesis of no difference between the OEF estimates made using the three different techniques. Post-hoc statistical testing was performed using the Tukey Kramer method (honest significant difference test) to test for differences between the estimates made using the different methods. A paired t-test was

used to test the null hypothesis of no difference between the DBV estimates made using sqBOLD and hyperoxia-BOLD.

Results

Table 2 displays $\Delta P_{ET}O_2$ and the change in end-tidal partial pressure of carbon dioxide ($\Delta P_{ET}CO_2$) during the hyperoxia-BOLD experiment for all participants. The mean $\Delta P_{ET}O_2$ was 294.7 mmHg and the mean $\Delta P_{ET}CO_2$ was 0.4 mmHg.

Figure 2 presents the results of the simulations of the sqBOLD and hqBOLD techniques. The R_2' estimated from the simulated qBOLD data is plotted against the true R_2' based on the pragmatic definition of DBV from above (Fig. 2a). A dashed line of unity is plotted and the slope of the relationship between the data is estimated as 0.99 (intercept -0.24 Hz). DBV_{sqBOLD} shows a large amount of uncertainty when compared with true DBV, which increases with true OEF (Fig. 2b). Whilst DBV_{hqBOLD} has a much lower uncertainty when OEF $\gtrsim$ 30 % (Fig. 2c). The slope of the relationship between DBV_{hqBOLD} and true DBV is 0.78 (intercept 0.05 %) for the full range of OEF values or 0.94 (intercept 0.01 %) when OEF > 30 %. OEF_{sqBOLD} does increase with true OEF, but has a very small dynamic range (Fig. 2d). Finally, OEF_{hqBOLD} increases monotonically with true OEF for OEF > 20 % with a dynamic range consistent with the full range of OEF (Fig. 2e).

Figure 3 presents simulations of the effect of system noise on measurements made using sqBOLD and hqBOLD. The true R_2' was estimated to be 2.8 s^{-1}, whilst the median value simulated was 2.3 s^{-1} (Fig. 3a). DBV_{sqBOLD} has an interquartile range (IQR) of 3.2 % (Fig. 3b), compared with the DBV_{hqBOLD} IQR of 0.27 % (Fig. 3c). The main difference in the sqBOLD and hqBOLD estimates of OEF is in their propensity for outliers, with the former having an excess kurtosis value of 17577.5 (Fig. 3d) and the latter a value of 0.1 (Fig. 3e).

Figure 4 shows parameter maps of DBV and OEF from sqBOLD and hqBOLD for three slices (slices 2, 5 and 8) in a single subject (sub-02). A single slice from each of the ten participants is provided in Figure S1. DBV_{hqBOLD} maps demonstrate an obvious contrast between GM and WM, with lower values in WM as expected. In the GM the OEF_{hqBOLD} maps show physiologically plausible values for healthy brain tissue. However, in WM unphysiological values of OEF are produced with a mean OEF value of 140.9 %. In comparison, the DBV_{sqBOLD} and OEF_{sqBOLD} maps demonstrate little contrast between GM and WM and agree well with the initial implementation of this method[3].

Table 3 shows regional estimates in GM extracted from hqBOLD and sqBOLD parameter maps. These estimates are compared to values of global OEF measured using TRUST. Group mean DBV_{hqBOLD} (1.8 ± 0.6 %) was found to be significantly different ($p<0.05$) to DBV_{sqBOLD} (3.9 ± 1.3 %). The one-way ANOVA was found to be significant ($p<0.001$) indicating that the mean OEF values for each group are not equal. Post-hoc pairwise comparisons revealed that OEF_{sqBOLD} is significantly different to OEF_{hqBOLD} ($p < 0.001$) and OEF_{TRUST} ($p < 0.001$), but that there was no significant difference between OEF_{hqBOLD} and OEF_{TRUST} ($p = 0.77$).

Figure 5 shows histograms of DBV_{hqBOLD}, OEF_{hqBOLD}, DBV_{sqBOLD} and OEF_{sqBOLD} voxel values within GM for one example participant (sub-03). These histograms show the distribution of voxel values that underlie the measurements presented in Table 3. DBV_{hqBOLD} exhibits a narrower distribution of voxel values compared to DBV_{sqBOLD} and OEF_{hqBOLD} displays a higher median OEF (Table 3) and a broader distribution of values compared to OEF_{sqBOLD}. Histograms for all ten participants are presented in Figure S2.

Figure 6 shows OEF_{TRUST} compared to OEF_{hqBOLD} and OEF_{sqBOLD}. Bland-Altman plots demonstrate a large bias between OEF_{TRUST} and OEF_{sqBOLD} of -24.3 percentage points

whereas OEF_{TRUST} and OEF_{hqBOLD} are in better agreement with a smaller bias of -2.4 points between techniques.

In order to understand the unphysiological OEF in WM, Table 4 compares the ratio of the GM to WM values of R_2', DBV_{sqBOLD} and DBV_{hqBOLD}. GM R_2' was found to be 22 % lower than WM, GM DBV_{sqBOLD} was found to be 29 % lower than WM and GM DBV_{hqBOLD} was found to be 234 % higher than WM.

Discussion

The aim of this study was to investigate whether an independent measure of DBV based on the hyperoxia-BOLD signal could improve the accuracy of qBOLD measurements of OEF. Simulations of this new technique, referred to here as hqBOLD, predicted a considerable improvement in estimates of both DBV and OEF compared with the existing sqBOLD technique. Experimentally, measurements of OEF acquired using hqBOLD and sqBOLD were compared with whole brain oximetry measurements from TRUST. The hqBOLD measurements of OEF were found to be in the range 23 to 53%, in good agreement with literature values of OEF in healthy cortical GM (~ 35 – 55 %)[40]. Whilst sqBOLD measurements of OEF were found to be systematically low (range 12 – 22 %) (Table 3). Furthermore, no significant difference was found between GM hqBOLD OEF measurements and TRUST OEF measurements (range 28 – 53 %).

Simulations

An accelerated Monte Carlo framework which scales and combines results from single vessel radius simulations was used to examine systematic and noise related errors. Simulations of the sqBOLD technique were consistent with previous results[8], namely that R_2' is linearly related to the true R_2' estimated from Eq. 3, that DBV_{sqBOLD} is a function of the OEF and this leads to a reduced dynamic range of OEF_{sqBOLD}. One difference between this

previous study and the current work is the definition of true DBV. As noted above, there isn't a strict definition of DBV because the level of deoxygenation varies across the vasculature and the way that deoxygenation is translated into the BOLD signal is affected by the vessel radius. Hence DBV can be pragmatically described as either all vessels containing deoxyhaemoglobin (capillaries + veins) or only venous vessels. The impact of moving from the former definition in the previous study to the latter in the current study is a greater correspondence between the simulated measurement of R_2' with the true R_2' (slope 0.99). This would suggest that the deoxygenated blood in the capillaries only makes a small contribution to the measured R_2'.

Simulations of DBV_{hqBOLD} provide an independent confirmation of the heuristic model (Eq. 8) for scaling the hyperoxia BOLD signal change to DBV. This heuristic was developed using an entirely different model to the one presented here based on analytical models of three vascular compartments[7]. In this previous work a narrower range of healthy OEF values were simulated (35 – 55 %). Despite this, Eq. 8 generalises well to the much larger OEF range simulated in this study (0 – 100 %), with minimal error in DBV_{hqBOLD} when OEF is greater than approximately 30 % (Fig. 2d). This is emphasised by the close correspondence between DBV_{hqBOLD} and true DBV with a slope of 0.95 for OEF > 30 % (Fig. 2c). Therefore, when combined with the simulated measurement of R_2' and Eq. 7, the dynamic range of OEF_{hqBOLD} is markedly improved.

Using noise levels estimated from the data, the simulations show that for a single physiological state the uncertainty in DBV_{sqBOLD} (Fig. 3b) is considerably larger than for DBV_{hqBOLD} (Fig. 3c). This might also explain the long tails and outliers for OEF_{sqBOLD} (Fig 3d and large excess kurtosis) as the reciprocal of the DBV distribution forms part of the OEF measurement (Eq. 9). When the shift of the distribution is small, or the uncertainty is large, the reciprocal of the distribution is bimodal and skewed. Hence negative values of OEF_{sqBOLD}

are observed and skewed for positive values, unlike OEF_{hqBOLD} where the uncertainty in DBV is lower.

Grey matter

Cortical GM measurements of DBV_{hqBOLD} (1.8±0.6 %) were significantly different ($p<0.05$) to DBV_{sqBOLD} derived measurements (3.9±1.3 %), with DBV_{sqBOLD} 2.2 times higher than DBV_{hqBOLD} on average. The sqBOLD measurements are consistent with previous implementations[3] (3.6±0.4 %), whilst the hqBOLD estimates are slightly lower than past measurements[7] (2.2±0.4 %). The hyperoxia-BOLD implementation in the current study differs in two ways from previous work: a shorter TR was used (down from 3 s to 1 s) and the hyperoxic gas mixture was presented differently. Automated gas delivery was used in this study, which benefits from isocapnic control and faster transitions between oxygen levels, compared with a two tube nasal cannula used in the previous study. An uncontrolled hyperoxic challenge, as in the latter case, can result in hyperventilation and associated hypocapnia[41]. However, hypocapnia should reduce the amplitude of the BOLD response to hyperoxia and hence we would expect the previous measurements to be lower than the current. Alternatively, a short TR could result in a decrease in the BOLD response to hyperoxia due to decrease in arterial blood T_1 due to the presence of paramagnetic oxygen dissolved in arterial blood plasma. However, detailed study of this issue has predicted that T_1 effects are negligible when compared with the changes in deoxyhaemoglobin elicited by hyperoxia[42].

Validation

The TRUST technique provides a way to measure whole brain OEF with few assumptions providing a way to benchmark sqBOLD and hqBOLD. Bland-Altman plots demonstrate that measurements of GM OEF made with hqBOLD agree well with TRUST oximetry across the group (Fig. 6b). The bias between the two methods was measured as -2.4 %. In contrast,

sqBOLD measures of OEF in GM demonstrate poor agreement and a large bias of -24.3 % when compared to TRUST oximetry (Fig. 6a).

White matter

The ratio of GM to WM DBV was measured as 0.7 for sqBOLD and 3.3 for hqBOLD. There are few studies in the literature that measure DBV quantitatively. A GM to WM DBV ratio of 2.29 was measured using qBOLD with the GESSE pulse sequence[2]. Alternatively, a study of CBVt measured a GM to WM CBVt ratio of 2.38. Both values are of a similar order to that measured using hyperoxia-BOLD in the current study. In contrast, DBV measured using sqBOLD in WM appears unphysiological given that it would suggest that WM has a higher vascular density than GM.

Under the assumptions: (i) that deoxyhaemoglobin is the dominant source of magnetic susceptibility in the voxel and (ii) that the blood vessels are uniformly and randomly distributed, Eq. (3) describes R_2' as a function of OEF and DBV. Furthermore, OEF is generally found to be the same in GM and WM in PET measurements[43]. Therefore, under these conditions the ratio of GM to WM R_2' would be expected to scale in the same way as DBV. Hence, we would expect the R_2' of GM to be 2.29 – 3.31 times higher than for WM, but the ratio was measured to be 0.78. A recent investigation of R_2' in WM has found that the two assumptions above are likely to be violated[44]. This study followed a multiparametric qBOLD approach whereby R_2' is estimated from maps of R_2 and R_2^* and estimated the angle between the primary eigenvector of WM voxels and B_0 using DTI. R_2' was found to increase as the angle increased. This orientation effect was considered by the authors to be a function of the preferential alignment of blood vessels parallel to WM fibre tracks and the magnetic susceptibility effects arising from the myelin rich WM fibres. Whilst orientation undoubtedly has a role at the voxel level, in the measurements presented in the current study this is likely to have been averaged out over the WM ROI. However, the additional magnetic susceptibility effect from myelin will remain and contribute to the measured R_2'.

Limitations and future work

It is worth noting some of the relevant limitations of the protocols used in this study. Firstly, the discrepancy in total acquisition time between sqBOLD (9:12 mins) and hqBOLD (29:12 mins) may at first glance appear to be an unfair comparison from an SNR perspective. However, as the simulations show, the underestimation of OEF is not due to a limitation in SNR but is caused by a systematic error. This study focussed on reducing this systematic error and future efforts will be directed towards reducing the overall scan duration.

The sqBOLD protocol used here has only minor differences compared with previous studies i.e. a slightly higher density of sampling at long τ values. We have shown that the long TE used here (TE = 80 ms) results in increased signal loss at the spin echo, due to the scale of the vessel distribution approaching the diffusion narrowing regime, causing DBV to be overestimated[8]. Unfortunately acquisition of the data in this study commenced before this simulation study had been completed and hence any improvements could not be implemented. Similarly, we have developed a Bayesian analysis tool for sqBOLD data, which has been shown to reduce the variance in parameter estimates[5]. However, since a tool to analyse the hqBOLD data in a Bayesian framework was not available, we chose to use least squares fitting for both techniques. However, we remain hopeful that an optimised sqBOLD protocol coupled with Bayesian model fitting can overcome some of the inaccuracy of the protocol used here.

The TRUST protocol used in this study had a longer echo time (7 ms) than recommended in a recent study[45] (3.6 ms). This has been shown to result in an overestimation of T_{2b} that leads to a slight overestimation in OEF of approximately 3-4%. However, this overestimation was shown to be dependent on image SNR and hence the number of averages acquired in this study was increased from the recommended number of three to four.

Conclusion

It has been shown by simulation and experiment that introducing an independent measure of DBV into the qBOLD framework provides improved estimates of OEF. Whilst mq-BOLD has previously used an independent measure of CBVt from DSC, this is not the relevant blood volume in the context of qBOLD. Hyperoxia-BOLD provides a quantitative and specific measure of DBV, such that the quantification of OEF is also improved. With further refinement this method has the potential to provide a clinically relevant measure of tissue oxygenation.

Appendix A

The code used to generate the simulation results can be downloaded from the Zenodo repository, doi: https://doi.org/10.5281/zenodo.14812818. The raw imaging data can be accessed via the Oxford Research Archive repository, doi: http://doi.org/10.5287/bodleian:X59eGb0pv. The code used to analyse these can be accessed via the Zenodo archive, doi: https://doi.org/10.5281/zenodo.14814607.

Appendix B: Supplementary data

Supplementary data to this article can be found online at <INSERT DOI TO SUPPLEMENTARY DATA>.

Acknowledgements

This work was supported by the Engineering and Physical Sciences Research Council [grant number EP/K025716/1].

References

1. An H, Lin W, Celik A, Lee YZ. Quantitative measurements of cerebral metabolic rate of oxygen utilization using MRI: A volunteer study. *NMR Biomed*. 2001;14(7-8):441-447. doi:10.1002/nbm.717

2. He X, Yablonskiy DA. Quantitative BOLD: Mapping of human cerebral deoxygenated blood volume and oxygen extraction fraction: Default state. *Magn Reson Med*. 2007;57(1):115-126. http://doi.wiley.com/10.1002/mrm.21108.
3. Stone AJ, Blockley NP. A streamlined acquisition for mapping baseline brain oxygenation using quantitative BOLD. *Neuroimage*. 2017;147(October 2016):79-88. doi:10.1016/j.neuroimage.2016.11.057
4. Stone AJ, Harston GWJ, Carone D, Okell TW, Kennedy J, Blockley NP. Prospects for investigating brain oxygenation in acute stroke: Experience with a non-contrast quantitative BOLD based approach. *Hum Brain Mapp*. 2019;40:2853-2866. doi:10.1002/hbm.24564
5. Cherukara MT, Stone AJ, Chappell MA, Blockley NP. Model-based Bayesian inference of brain oxygenation using quantitative BOLD. *Neuroimage*. 2019;202:116106. doi:10.1016/j.neuroimage.2019.116106
6. An H, Lin W. Impact of intravascular signal on quantitative measures of cerebral oxygen extraction and blood volume under normo- and hypercapnic conditions using an asymmetric spin echo approach. *Magn Reson Med*. 2003;50(4):708-716. http://doi.wiley.com/10.1002/mrm.10576.
7. Blockley NP, Griffeth VEM, Germuska MA, Bulte DP, Buxton RB. An analysis of the use of hyperoxia for measuring venous cerebral blood volume: Comparison of the existing method with a new analysis approach. *Neuroimage*. 2013;72:33-40. http://linkinghub.elsevier.com/retrieve/pii/S1053811913000864.
8. Stone AJ, Holland NC, Berman AJL, Blockley NP. Simulations of the effect of diffusion on asymmetric spin echo based quantitative BOLD: An investigation of the origin of deoxygenated blood volume overestimation. *Neuroimage*. 2019;201(March):116035. doi:10.1016/j.neuroimage.2019.116035
9. Christen T, Lemasson B, Pannetier N, et al. Evaluation of a quantitative blood oxygenation level-dependent (qBOLD) approach to map local blood oxygen saturation. *NMR Biomed*. 2010;24(4):393-403. http://eutils.ncbi.nlm.nih.gov/entrez/eutils/elink.fcgi?dbfrom=pubmed&id=20960585&retmode=ref&cmd=prlinks.
10. Tóth V, Förschler A, Hirsch NM, et al. MR-based hypoxia measures in human glioma. *J Neurooncol*. 2013;115(2):197-207. http://link.springer.com/10.1007/s11060-013-1210-7.
11. Rempp KA, Brix G, Wenz F, Becker CR, Gückel F, Lorenz WJ. Quantification of regional cerebral blood flow and volume with dynamic susceptibility contrast-enhanced MR imaging. *Radiology*. 1994;193(3):637-641. http://eutils.ncbi.nlm.nih.gov/entrez/eutils/elink.fcgi?dbfrom=pubmed&id=7972800&retmode=ref&cmd=prlinks.
12. Lu H, Ge Y. Quantitative evaluation of oxygenation in venous vessels using T2-Relaxation-Under-Spin-Tagging MRI. *Magn Reson Med*. 2008;60(2):357-363. http://doi.wiley.com/10.1002/mrm.21627.
13. Boxerman JL, Hamberg LM, Rosen BR, Weisskoff RM. MR contrast due to intravascular magnetic susceptibility perturbations. *Magn Reson Med*. 1995;34(4):555-566. http://eutils.ncbi.nlm.nih.gov/entrez/eutils/elink.fcgi?dbfrom=pubmed&id=8524024&retmode=ref&cmd=prlinks.
14. Blockley NP, Jiang L, Gardener AG, Ludman CN, Francis ST, Gowland PA. Field strength dependence of R 1 and R2* relaxivities of human whole blood to prohance, vasovist, and deoxyhemoglobin. *Magn Reson Med*. 2008;60(6):1313-1320. doi:10.1002/mrm.21792
15. Kiselev VG, Posse S. Analytical model of susceptibility-induced MR signal dephasing: effect of diffusion in a microvascular network. *Magn Reson Med*. 1999;41(3):499-509. http://eutils.ncbi.nlm.nih.gov/entrez/eutils/elink.fcgi?dbfrom=pubmed&id=10204873&retmode=ref&cmd=prlinks.

16. Dickson JD, Ash TWJ, Williams GB, Sukstanskii AL, Ansorge RE, Yablonskiy DA. Quantitative phenomenological model of the BOLD contrast mechanism. *J Magn Reson*. 2011;212(1):17-25. http://eutils.ncbi.nlm.nih.gov/entrez/eutils/elink.fcgi?dbfrom=pubmed&id=21782488&retmode=ref&cmd=prlinks.
17. Sharan M, Jones MD, Koehler RC, Traystman RJ, Popel AS. A compartmental model for oxygen transport in brain microcirculation. *Ann Biomed Eng*. 1989;17(1):13-38. http://link.springer.com/10.1007/BF02364271.
18. Berman AJL, Mazerolle EL, MacDonald ME, Blockley NP, Luh WM, Pike GB. Gas-free calibrated fMRI with a correction for vessel-size sensitivity. *Neuroimage*. 2018;169:176-188.
19. Berman AJL, Pike GB. Transverse signal decay under the weak field approximation: Theory and validation. *Magn Reson Med*. 2018;80(1):341-350. doi:10.1002/mrm.27035
20. Severinghaus JW. Simple, accurate equations for human blood O2 dissociation computations. *J Appl Physiol Respir Environ Exerc Physiol*. 1979;46(3):599-602. http://eutils.ncbi.nlm.nih.gov/entrez/eutils/elink.fcgi?dbfrom=pubmed&id=35496&retmode=ref&cmd=prlinks.
21. Griffeth VEM, Buxton RB. A theoretical framework for estimating cerebral oxygen metabolism changes using the calibrated-BOLD method: Modeling the effects of blood volume distribution, hematocrit, oxygen extraction fraction, and tissue signal properties on the BOLD signal. *Neuroimage*. 2011;58(1):198-212. http://eutils.ncbi.nlm.nih.gov/entrez/eutils/elink.fcgi?dbfrom=pubmed&id=21669292&retmode=ref&cmd=prlinks.
22. Tsai AG, Johnson PC, Intaglietta M. Oxygen gradients in the microcirculation. *Physiol Rev*. 2003;83(3):933-963. http://eutils.ncbi.nlm.nih.gov/entrez/eutils/elink.fcgi?dbfrom=pubmed&id=12843412&retmode=ref&cmd=prlinks.
23. Blockley NP, Griffeth VEM, Buxton RB. A general analysis of calibrated BOLD methodology for measuring CMRO2 responses: Comparison of a new approach with existing methods. *Neuroimage*. 2012;60(1):279-289. doi:10.1016/j.neuroimage.2011.11.081
24. *Determination of Signal-to-Noise Ratio (SNR) in Diagnostic Magnetic Resonance Imaging*. Rosslyn, VA; 2021. www.nema.org.
25. Ogawa S, Menon RS, Tank DW, et al. Functional brain mapping by blood oxygenation level-dependent contrast magnetic resonance imaging. A comparison of signal characteristics with a biophysical model. *Biophys J*. 1993;64(3):803-812. http://eutils.ncbi.nlm.nih.gov/entrez/eutils/elink.fcgi?dbfrom=pubmed&id=8386018&retmode=ref&cmd=prlinks.
26. Spees WM, Yablonskiy DA, Oswood MC, Ackerman JJ. Water proton MR properties of human blood at 1.5 Tesla: magnetic susceptibility, T1, T2, T2*, and non-Lorentzian signal behavior. *Magn Reson Med*. 2001;45(4):533-542. http://eutils.ncbi.nlm.nih.gov/entrez/eutils/elink.fcgi?dbfrom=pubmed&id=11283978&retmode=ref&cmd=prlinks.
27. Blockley NP, Stone AJ. Improving the specificity of R2′ to the deoxyhaemoglobin content of brain tissue: Prospective correction of macroscopic magnetic field gradients. *Neuroimage*. 2016;135:253-260. doi:10.1016/j.neuroimage.2016.04.013
28. Hajnal J v, Bryant DJ, Kasuboski L, et al. Use of fluid attenuated inversion recovery (FLAIR) pulse sequences in MRI of the brain. *J Comput Assist Tomogr*. 1992;16(6):841-844. http://eutils.ncbi.nlm.nih.gov/entrez/eutils/elink.fcgi?dbfrom=pubmed&id=1430427&retmode=ref&cmd=prlinks.
29. Mugler JP, Brookeman JR. Three-dimensional magnetization-prepared rapid gradient-echo imaging (3D MP RAGE). *Magn Reson Med*. 1990;15(1):152-157.

http://eutils.ncbi.nlm.nih.gov/entrez/eutils/elink.fcgi?dbfrom=pubmed&id=2374495&retmode=ref&cmd=prlinks.

30. Jenkinson M, Beckmann CF, Behrens TEJ, Woolrich MW, Smith SM. FSL. *Neuroimage*. 2012;62(2):782-790. http://dx.doi.org/10.1016/j.neuroimage.2011.09.015.

31. Peng SL, Dumas JA, Park DC, et al. Age-related increase of resting metabolic rate in the human brain. *Neuroimage*. May 2014:1-8. http://dx.doi.org/10.1016/j.neuroimage.2014.04.078.

32. Lu H, Xu F, Grgac K, Liu P, Qin Q, van Zijl PCM. Calibration and validation of TRUST MRI for the estimation of cerebral blood oxygenation. *Magn Reson Med*. 2012;67(1):42-49. http://eutils.ncbi.nlm.nih.gov/entrez/eutils/elink.fcgi?dbfrom=pubmed&id=21590721&retmode=ref&cmd=prlinks.

33. Jenkinson M, Bannister P, Brady M, Smith S. Improved optimization for the robust and accurate linear registration and motion correction of brain images. *Neuroimage*. 2002;17(2):825-841. http://eutils.ncbi.nlm.nih.gov/entrez/eutils/elink.fcgi?dbfrom=pubmed&id=12377157&retmode=ref&cmd=prlinks.

34. Smith SM. Fast robust automated brain extraction. *Hum Brain Mapp*. 2002;17(3):143-155. http://doi.wiley.com/10.1002/hbm.10062.

35. Yablonskiy DA, Haacke EM. Theory of NMR signal behavior in magnetically inhomogeneous tissues: the static dephasing regime. *Magn Reson Med*. 1994;32(6):749-763. http://eutils.ncbi.nlm.nih.gov/entrez/eutils/elink.fcgi?dbfrom=pubmed&id=7869897&retmode=ref&cmd=prlinks.

36. Eichling JO, Raichle ME, Grubb RL, Larson KB, Ter-Pogossian MM. In vivo determination of cerebral blood volume with radioactive oxygen 15 in the monkey. *Circ Res*. 1975;37(6):707-714. doi:10.1161/01.RES.37.6.707

37. Jenkinson M, Smith S. A global optimisation method for robust affine registration of brain images. *Med Image Anal*. 2001;5(2):143-156. doi:10.1016/S1361-8415(01)00036-6

38. Zhang Y, Brady M, Smith S. Segmentation of brain MR images through a hidden Markov random field model and the expectation-maximization algorithm. *IEEE Trans Med Imaging*. 2001;20(1):45-57. http://eutils.ncbi.nlm.nih.gov/entrez/eutils/elink.fcgi?dbfrom=pubmed&id=11293691&retmode=ref&cmd=prlinks.

39. Mazziotta J, Toga A, Evans A, et al. A probabilistic atlas and reference system for the human brain: International Consortium for Brain Mapping (ICBM). *Philos Trans R Soc Lond B Biol Sci*. 2001;356(1412):1293-1322. http://eutils.ncbi.nlm.nih.gov/entrez/eutils/elink.fcgi?dbfrom=pubmed&id=11545704&retmode=ref&cmd=prlinks.

40. Marchal G, Rioux P, Petit-Taboué MC, et al. Regional cerebral oxygen consumption, blood flow, and blood volume in healthy human aging. *Arch Neurol*. 1992;49(10):1013-1020. http://eutils.ncbi.nlm.nih.gov/entrez/eutils/elink.fcgi?dbfrom=pubmed&id=1417508&retmode=ref&cmd=prlinks.

41. Iscoe S, Fisher JA. Hyperoxia-induced hypocapnia: an underappreciated risk. *Chest*. 2005;128(1):430-433. http://eutils.ncbi.nlm.nih.gov/entrez/eutils/elink.fcgi?dbfrom=pubmed&id=16002967&retmode=ref&cmd=prlinks.

42. Ma Y, Berman AJL, Pike GB. The effect of dissolved oxygen on the relaxation rates of blood plasma: Implications for hyperoxia calibrated BOLD. *Magn Reson Med*. December 2015:n/a-n/a. http://doi.wiley.com/10.1002/mrm.26069.

43. Cho J, Lee J, An H, Goyal MS, Su Y, Wang Y. Cerebral oxygen extraction fraction (OEF): Comparison of challenge-free gradient echo QSM+qBOLD (QQ) with 15O

PET in healthy adults. *Journal of Cerebral Blood Flow and Metabolism*. 2021;41(7):1658-1668. doi:10.1177/0271678X20973951

44. Kaczmarz S, Göttler J, Zimmer C, Hyder F, Preibisch C. Characterizing white matter fiber orientation effects on multi-parametric quantitative BOLD assessment of oxygen extraction fraction. *Journal of Cerebral Blood Flow and Metabolism*. 2020;40(4):760-774. doi:10.1177/0271678X19839502

45. Xu F, Uh J, Liu P, Lu H. On improving the speed and reliability of T2-relaxation-under-spin-tagging (TRUST) MRI. *Magn Reson Med*. 2012;68(1):198-204. http://onlinelibrary.wiley.com/doi/10.1002/mrm.23207/full.

Figure Captions

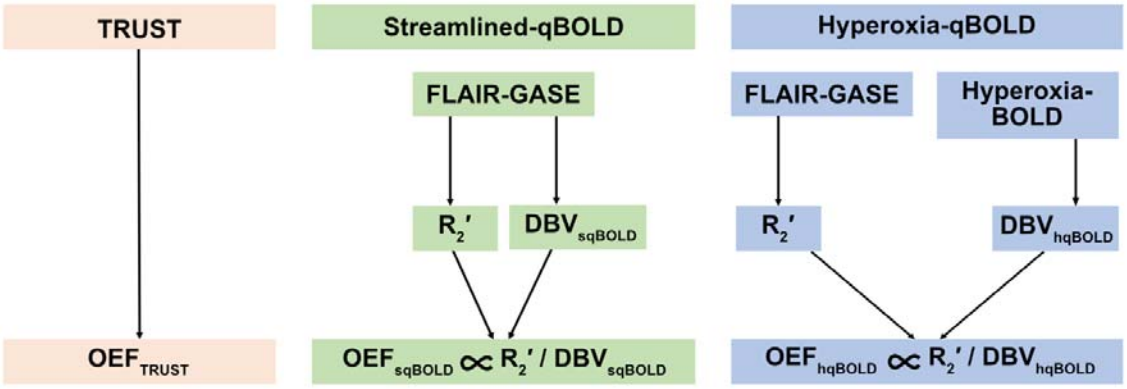

Figure 1: Schematic outlining the MR / physiological parameters derived from each imaging method which include the TRUST (T_2 relaxation under spin tagging) method for measuring whole brain oxygen extraction fraction (OEF), the streamlined-qBOLD technique for mapping tissue OEF and deoxygenated blood volume (DBV) and the hyperoxia-qBOLD approach which uses an independent measurement of DBV from hyperoxia BOLD to map OEF.

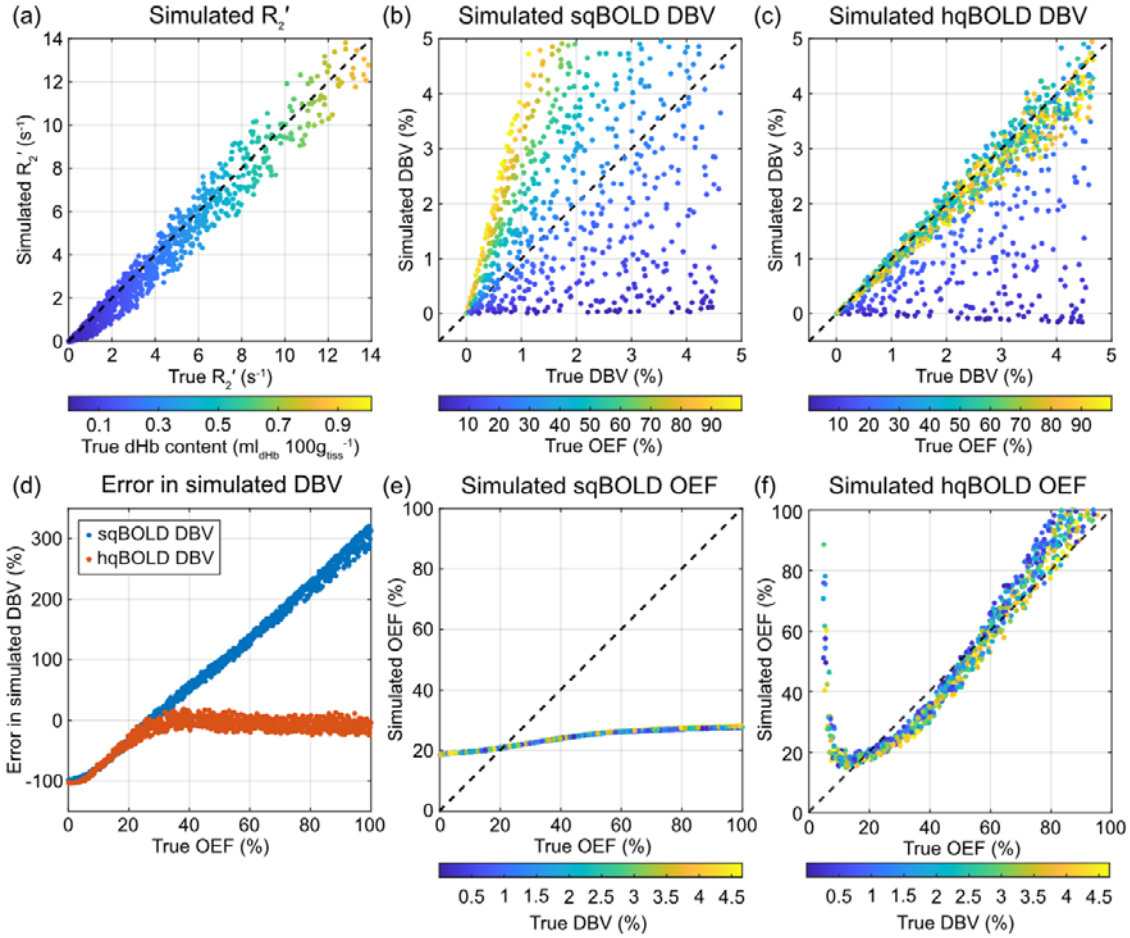

Figure 2: Simulations of the systematic error in the two qBOLD approaches. (a) simulated R_2' compared with 'true' R_2' calculated using the static dephasing qBOLD model, (b-c) simulated streamlined-qBOLD (sqBOLD) DBV and hyperoxia-BOLD (hqBOLD) DBV vs true DBV, respectively, (d) error in simulated DBV for sqBOLD and hqBOLD techniques and (e-f) simulated OEF from sqBOLD and hqBOLD, respectively.

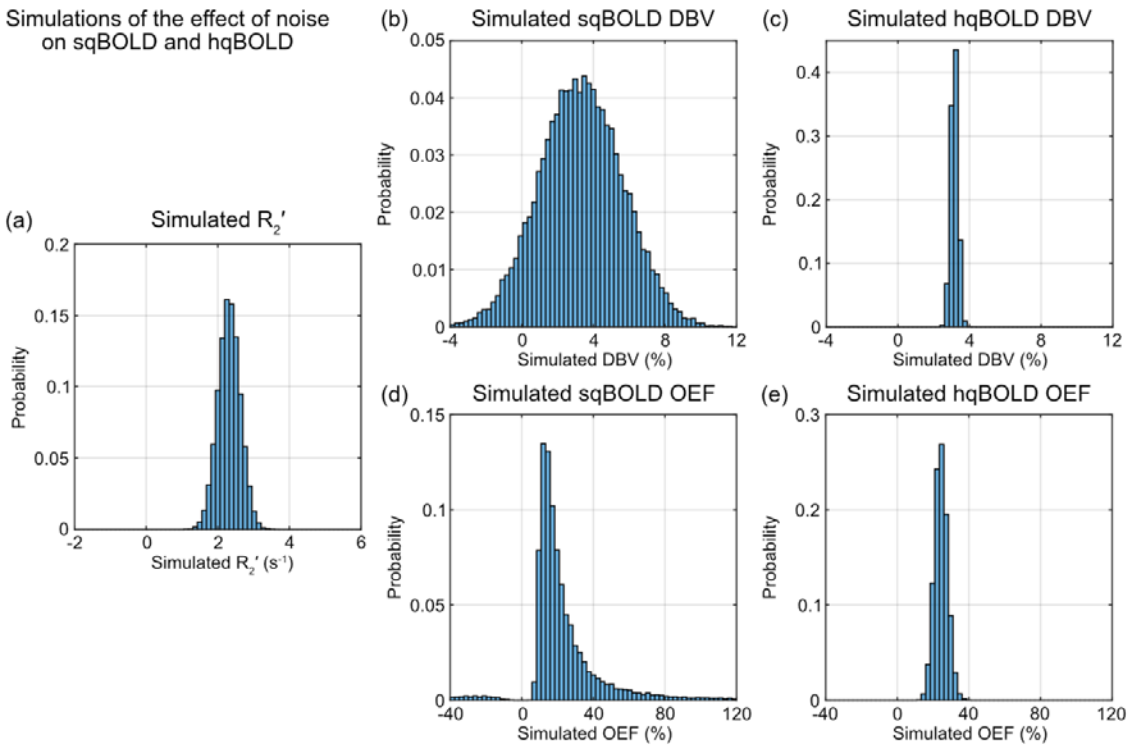

Figure 3: Simulations of the effect of noise for the two qBOLD approaches. (a) the distribution of R_2' values estimated from simulated qBOLD signals, (b-c) the distribution of deoxygenated blood volume (DBV) values for streamlined-qBOLD (sqBOLD) and hyperoxia-qBOLD (hqBOLD) techniques, respectively, and (d-e) the distribution of oxygen extraction fraction (OEF) values for sqBOLD and hqBOLD, respectively.

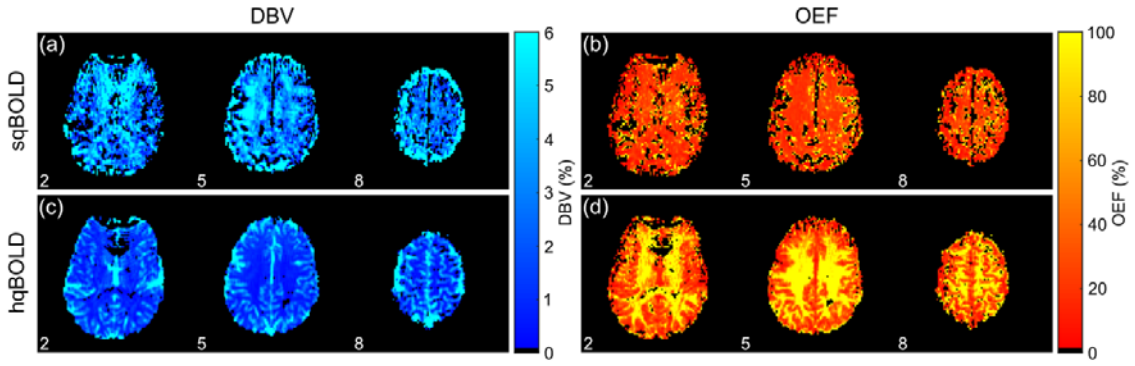

Figure 4: Example maps of deoxygenated blood volume (DBV) and oxygen extraction fraction (OEF) from the (a-b) the streamlined-qBOLD (sqBOLD) technique and (c-d) the hyperoxia-qBOLD (hqBOLD) method.

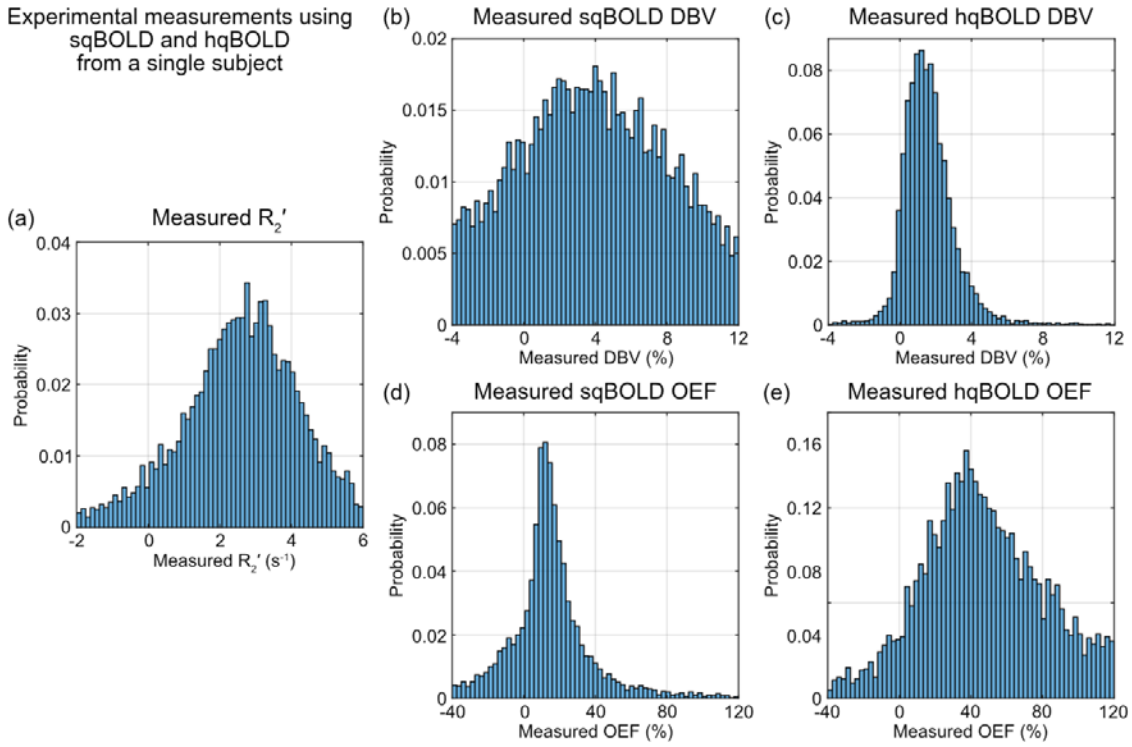

Figure 5: Histograms of experimental qBOLD measurements in grey matter. (a) the distribution of R_2' values, (b-c) the distribution of deoxygenated blood volume (DBV) values for streamlined-qBOLD (sqBOLD) and hyperoxia-qBOLD (hqBOLD) techniques, respectively, and (d-e) the distribution of oxygen extraction fraction (OEF) values for sqBOLD and hqBOLD, respectively.

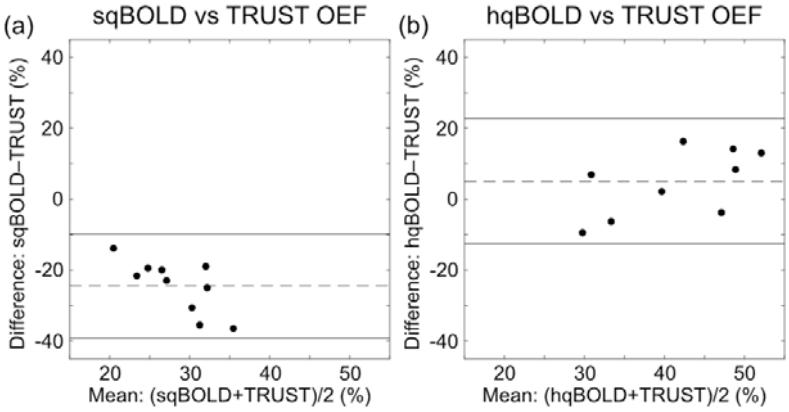

Figure 6: Bland-Altman plot comparing hyperoxia-qBOLD (hqBOLD) measures of oxygen extraction fraction (OEF) in global grey matter with streamlined-qBOLD (sqBOLD) and TRUST (T_2 relaxation under spin tagging) measures of OEF.

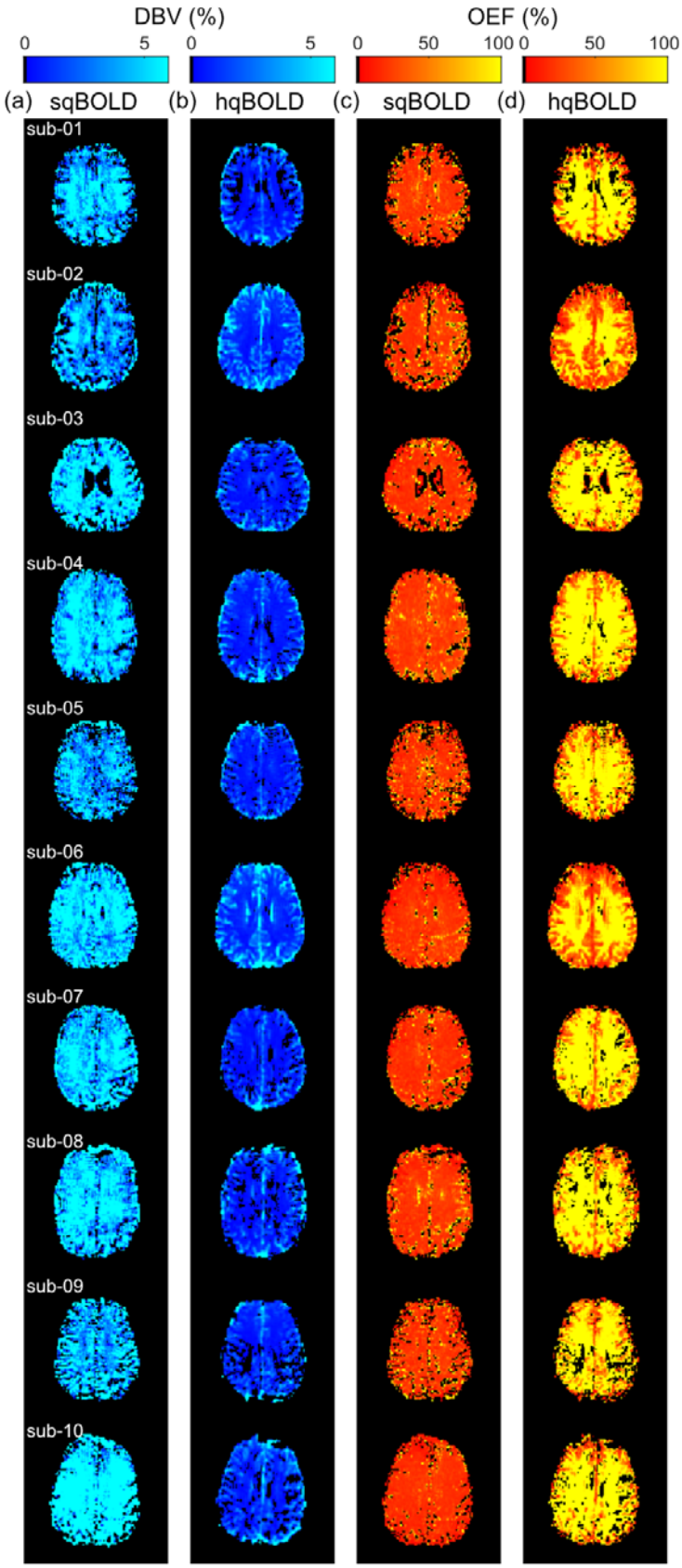
DBV (%)
0
5
0
5
OEF (%)
0
50
100
0
50
100
(a) sqBOLD
(b) hqBOLD
(c) sqBOLD
(d) hqBOLD
sub-01
sub-02
sub-03
sub-04
sub-05
sub-06
sub-07
sub-08
sub-09
sub-10

722

Figure S1: A single slice of the streamlined-qBOLD (sqBOLD) and hyperoxia-qBOLD (hqBOLD) data of each of the participants. (a-b) deoxygenated blood volume (DBV) and (c-d) oxygen extraction fraction (OEF) maps.

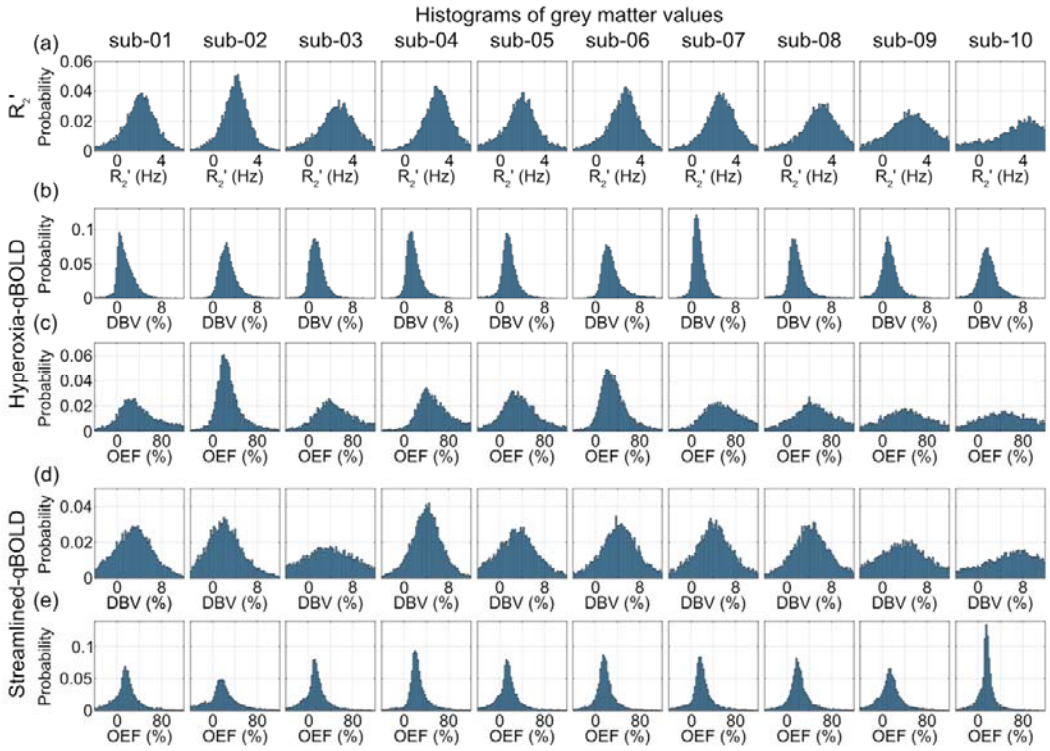

Figure S2: Histograms of experimental qBOLD measurements in grey matter for all subjects. (a) the distribution of R_2' values, (b-c) the distribution of deoxygenated blood volume (DBV) and oxygen extraction fraction (OEF) values for hyperoxia-qBOLD (hqBOLD) and (d-e) the distribution of DBV and OEF values for streamlined-qBOLD (sqBOLD).

Parameter	Standard Value	Range tested	Description
CBVt	5 %	0 – 10 %	Total cerebral blood volume
OEF	40 %	0 – 100 %	Oxygen extraction fraction
Hct	34 %	31 – 43 %	Small vessel haematocrit
PaO_2^{norm}	110 mmHg	100 – 130 mmHg	Normoxic arterial partial pressure of oxygen
PaO_2^{hyper}	400 mmHg	370 – 450 mmHg	Hyperoxic arterial partial pressure of oxygen

Table 1: Simulation parameters used to define the physiological state. The standard value was used when investigating the effect of noise and the range tested reflects the ranges used to investigate systematic error.

Subject	$P_{ET}O_2$ (mmHg)	$\Delta P_{ET}O_2$ (mmHg)	$P_{ET}CO_2$ (mmHg)	$\Delta P_{ET}CO_2$ (mmHg)
sub-01	122.9	321.5	34.9	1.0
sub-02	108.9	277.8	41.7	1.2
sub-03	109.8	295.6	43.3	0.5
sub-04	109.2	297.0	41.3	-0.2
sub-05	104.9	291.0	39.6	-0.1
sub-06	109.3	268.2	39.5	2.3
sub-07	112.0	296.9	36.3	-0.5
sub-08	128.8	312.6	35.4	0.5
sub-09	128.8	277.7	37.0	0.6
sub-10	109.0	308.7	42.2	-1.1
Mean	114.4	294.7	39.1	0.4
SD	8.9	16.8	3.0	1.0

Table 2: Parameter estimates of deoxygenated blood volume (DBV) and oxygen extraction fraction (OEF) calculated using streamlined-qBOLD (sqBOLD), hyperoxia-qBOLD (hqBOLD) and T_2 relaxation under spin tagging (TRUST). Median values in global grey matter are shown for each subject and presented alongside the group mean and standard deviation.